PCCP

Accepted Manuscript




ROYAL SOCIETY OF CHEMISTRY

www.rsc.org/pccp

Journal Name

RSCPublishing

COMMUNICATION

# Soft Nano Wrapping on Graphene Oxide by using Metal-organic Network Composed of Tannic Acid and Fe Ions

Cite this: DOI: 10.1039/x0xx00000x

Received ooth January 2012,
Accepted ooth January 2012

DOI: 10.1039/x0xx00000x

www.rsc.org/

H. Ozawa,*[a] and M. Haga*[a]

**Graphene oxide (GO) nanosheets were easily covered with uniform metal-organic network films composed of tannic acid and Fe ions. The surface morphology of the wrapped GO sheets was elucidated by atomic force, scanning electron, and transmission electron microscopy measurements. The GO sheets covered with the TA-Fe films on a substrate were reduced chemically without the collapse of the wrapped nanostructure of the TA-Fe/GO sheets. The modified GO sheets covered with TA-Fe were highly stable in water and easy to handle, which made it possible to place on microelectrode array for conductivity measurement.**

Two-dimensional (2D) carbon nanomaterials, such as graphene oxide (GO), reduced graphene oxide (rGO), and graphene, have gained considerable attention as potential materials for various applications because of their unique structures and electronic properties.[1-4] Recently, various assemblies based on GO and graphene have also become an active area of research.[4-6] A simple and effective method of preparing multilayer films composed of molecular building blocks with GO or graphene is a requisite for introducing various functionalities into material science. Therefore, the composites of carbon nanomaterials with metal-organic networks of nanometer-sized thickness and uniformity over large areas have the potential as next generation composite materials for sensing devices, solar cells, supercapacitors, nano-electronic devices, and field effect transistors. [7-15]

Recently, natural materials have become of interest due to their abundance in nature. In a sustainable society, use of natural compounds as new materials has the advantage of enabling construction of environment load reduction systems in various industrial, biomedical, and pharmacological fields.[16-19] Tannic acid (TA) is one such material and has a unique structure that contains a number of pyrogallol hydroxyls that have high affinity and a combination of hydrogen bonding, hydrophobic interactions, electrostatic interaction, and strong chelating ability to various metal ions.[20]

Ejima et al. recently reported on simple and rapid one-step fabrication of multi-layer films assembled on a variety of substrate surfaces via the coordination bonding between TA and $Fe^{III}$ ions. They succeeded in coating various planar and particulate substrates such as glass, gold, polymers, and silica.[21] They also succeeded in the preparation of multi-functional capsules through coordination of different metal ions and TA for drug delivery.[22, 23] Tannic acid also has a unique reducing property and acts as a mild reducing agent. By using this reducing poperty, Lei et al. successfully converted GO to reduced GO (rGO). The mixture of rGO with TA became soluble in various solvents due to hydrophilicity after the mixing of hydrophobic rGO with TA.[24] Additionally, some research groups reported on the synthesis of metal nanoparticles concurrently with the reduction of GO by TA. Therefore, GO and rGO modification by TA is used to fabricate various new nanomaterials such as catalysis and energy storage materials.[25-28]

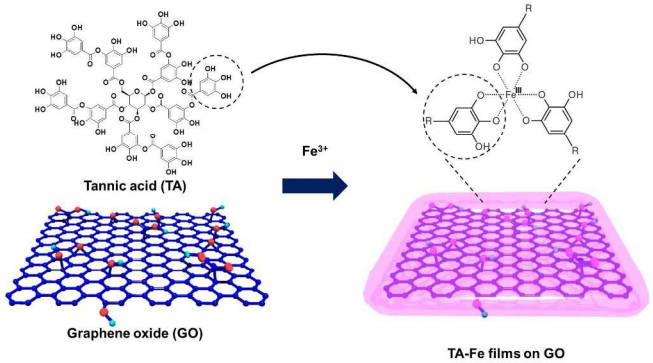


Scheme 1. Preparation scheme of TA-Fe films covered GO sheet.

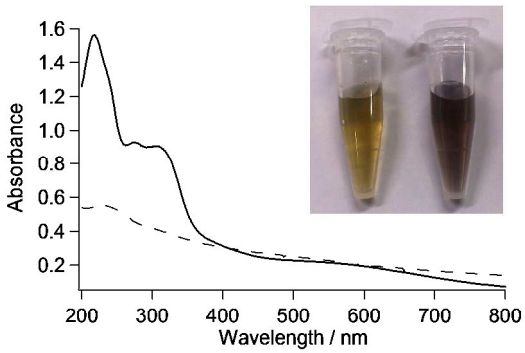


Figure 1. UV-Vis absorption spectra of TA-Fe/GO (solid line) and GO (broken line). Inset; photograph of TA-Fe/GO (right) and GO (left).

We report on a soft wrapping method for GO sheets covered with uniform $Fe^{III}$-TA metal-organic network films by the complex formation of TA and $Fe^{III}$ ions. Moreover, the chemical reduction of GO-covered TA-Fe films by hydrazine hydrate led to rGO maintaining the wrapping structures with TA-Fe film. The obtained composite sheets from TA and $Fe^{III}$ ions on GO, abbreviated as TA-Fe/GO sheets and their chemically reduced TA-Fe/rGO sheets, were characterized using physical measurements and electron microscopy techniques.

Scheme 1 shows a preparation method of TA-Fe/GO sheets. Graphene oxide was prepared from graphite flakes by using the improved Hummer's method.[29] Since the surface of GO is known to exhibit various types of defects with oxygen-containing functional groups, it can be easily modified with various materials using these defect sites. Furthermore, GO was chemically reduced to rGO, resulting in highly conductive materials. Therefore, we selected GO to develop a new building block for the bottom-up fabrication of nanomaterials. The TA-Fe films were prepared using the following method by Ejima et al.[21] Since this method of preparing TA-Fe films

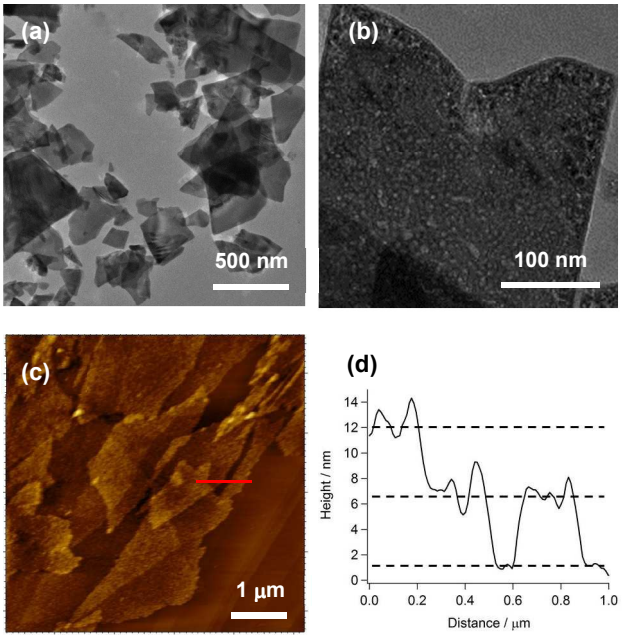


Figure 2. (a) TEM images and (b) magnification of TA-Fe/GO sheets. (c) AFM image and (d) cross section of TA-Fe/GO sheets on HOGP substrate. Red line shows location of cross section.

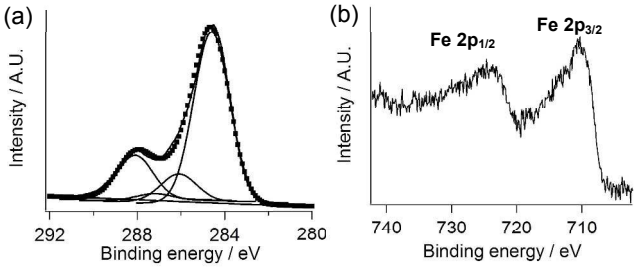


Figure 3. XPS 1Cs (a) and Fe 2p (b) spectra of TA-Fe/GO sheets on silicon substrates.

is simple and versatile, GO sheets can be easily wrapped with TA-Fe films by just the addition of $Fe^{III}$ ions into the GO solution containing TA. The structure of TA-Fe film is known as the $Fe^{III}$-TA coordination polymer, which is a similar structure to analogous $Fe^{III}$-catechol complexes.[21] For the formation TA-Fe film on GO, several interactions between GO and TA-Fe films will be included such as the multiple-point hydrogen bonding, the coordination bond between Fe and OH, COOH groups in GO, and weak π-π interaction between tannic acid and GO.

UV-Vis absorption spectra of TA-Fe/GO and GO are shown in Figure 1. Two peaks of TA-Fe/GO were observed at 218 and 275 nm, which corresponds to the π-π* and n-π* transitions of TA, respectively. Other peaks appeared at 308 and 550 nm. The peak at 308 nm was assigned to the TA absorption peaks coordinated to the $Fe^{III}$ ions, and the broad peak around 550 nm corresponds to a coordinated TA to $Fe^{III}$-charge transfer band in the $Fe^{III}$-TA coordination compound. The solution color arising from the $Fe^{III}$-TA coordination compound was pH-dependent.[21] We measured the UV-Vis absorption spectra of the TA-Fe/GO sheet under base and acid conditions (Figure S1). For the base condition, the peak red-shifted from 308 to 317 nm. These spectral changes were consistent with the intraligand transitions of TA pyrogallol moieties by the deprotonation on coordinated $Fe^{III}$ -TA moieties.[21] On the other hand, for the acid condition, the peak above 300 nm disappeared because TA-Fe structures are easily broken.[21]

To further invesitgate the surface properties of the TA-Fe/GO composite, zeta potentials were measured before and after the wrapping of the GO sheets. Upon wrapping the GO sheets, the surface zeta potential decreased from –35.8 ± 0.3 mV to –43.8 ± 0.8 mV due to the incrase in the negative charge by free galloyl groups of TA. We measured the size of the GO sheets by dynamic light scattering (DLS) method before and after the wrapping of GO sheets with the TA-Fe film. The average diameter of the GO sheets was changed from 3.5 μm to 1.8 μm. The results implied that TA-Fe film coating prevents the aggregations of GOs. Figure 2a shows a transmission electron microscopy (TEM) image of the TA-Fe/GO sheets. The sheet structures were observed, indicating the preservation of the GO sheet structure. However, overlapping between the GO sheets and their aggregation was partially observed. The magnified TEM image of the TA-Fe/GO sheets showed a ragged surface morphology of TA-Fe/GO, indicating nanometer-sized wrapping by the TA-Fe networked films. The scanning electron microscopy (SEM) image of the TA-Fe/GO sheets also showed ragged structures on them, as shown in Figure S2. Furthermore, the surface morphology of the TA-Fe/GO sheets on a highly ordered pyrolytic graphite (HOPG) substrate was observed using atomic force microscopy (AFM) (Figure 2c). According to the AFM image of the TA-Fe/GO sheets, the lateral size of the sheets was in sub-micrometers and the surface of the sheets became ragged

compared to that of the GO sheet (Figure S3). From a cross section analysis, their average thickness was about 5 nm (Figure 2d), which is thicker than that for the reported height of bare GO (~ 1 nm). These results indicated that the TA-Fe/GO composite film was covered with TA-Fe network films.

The elemental analyses of the GO sheet itself, GO sheet wrapped by TA-Fe films were carried out. The C, H, and O percentage ratios of GO were 44.84, 2.44 and 52.72%, respectively. The C and H percentage ratios of TA-Fe/GO were 40.31 and 2.50% and the remaining ratio was 57.19%, which contained the elements O and Fe. Since the C, H, and O percentage ratios of TA are 53.66, 3.08, and 43.26%, it can be predicted that the C ratio of the sample was increased by the reduction of GO and TA wrapping. However, the C ratio of TA-Fe/GO was decreased, indicating the existence of Fe in the films. The FT-IR spectra of TA, GO, and TA-Fe/GO are shown in Figure S4. The peak at 760 $cm^{-1}$ observed in the spectra of TA and TA-Fe/GO corresponds to multi-substituted aromatic rings in TA, indicating the presence of TA in the structures. After the formation of TA-Fe films, the peak at 1448 $cm^{-1}$, which corresponds to C–O–H in plane bending mode of the hydroxyl groups in TA, was weakened because of the complex formation between hydroxyl groups in TA and Fe.[30] The Raman spectra of the TA-Fe/GO and GO sheets were measured and are shown in Figure S5. It is known that GO sheets show the G band at around 1600 $cm^{-1}$ and D band at around 1350 $cm^{-1}$, which are attributed to the in-plane bonding stretching motion of pairs of $sp^2$ carbon atoms and the structural defects created by the hydroxyl and epoxide groups on the carbon basal plane, respectively.

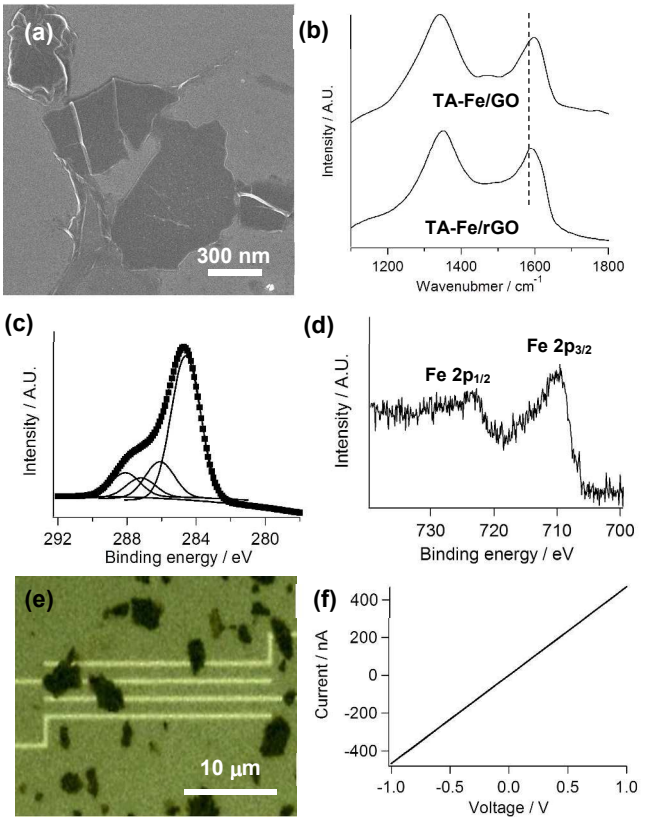


Figure 4. (a) SEM image of TA-Fe/rGO sheets on silicon substrate. (b) Raman spectra of TA-Fe/rGO and TA-Fe/GO sheets. Broken line shows peak apex of D band of TA-Fe/rGO sheets on silicon substrate. (c) XPS C 1s and (d) Fe 2p spectra of TA-Fe/rGO sheets on silicon substrates. (e) Photograph and (f) I-V curve of TA-Fe/rGO between gold electrodes. Gap between electrodes was 2 μm.

For the GO sample for our study, these two peaks appeared at 1346 and 1595 $cm^{-1}$, respectively. After the wrapping of GO, these two D and G bands of TA-Fe/GO were observed at 1342 and 1597 $cm^{-1}$, respectively, which are almost the same wavelengths as those of the original GO sheet. This small shift in the two peaks may be due to the partial reduction to graphene by TA.

X-ray photoelectron spectroscopy (XPS) measurement was carried out to further characterize TA-Fe/GO on a silicon substrate (Figure 3 and S6). As shown in Figure S6, C1s, O1s, Fe $2p_{1/2}$, and Fe $2p_{3/2}$ peaks were observed at 284.6, 531.4, 710.4, and 723.8 eV, respectively. Two peaks from Fe 2p revealed the presence of Fe species in TA-Fe/GO. For carbon atoms, those four peaks at 284.6, 286.1, 287.2, and 288.1 eV were assigned to the carbon 1s signals originating from C=C, C-O, C=O, and O-C=O moieties, respectively, from the peak deconvolution results. The line shape of the C1s peak of TA-Fe/GO changed significantly compared to those of the bare GO sheet (Figure S7). The remarkable decrease in intensity of the peak assigned to C-O at 286.1 eV after the formation of the TA-Fe/GO composite indicated that partial reduction of GO took place during the preparation of the composite since TA-bearing pyrogallol groups are known to act as reducing agents.[24]

The further reduction of TA-Fe/GO sheets on Si substrates was carried out using a general method involving hydrazine vapor.[31] The TA-Fe/rGO sheets were verified by SEM measurements, UV-Vis absorption, Raman, XPS spectroscopy, and thermogravimetric analysis (TG) analysis. The SEM image of the TA-Fe/rGO sheets is shown in Figure 4a. The sheet structures were clearly observed in the SEM image even after reduction, and the reduction did not affect the sheet structure and size of the TA-Fe/GO sheets. The UV-Vis absorption spectrum of TA-Fe/rGO sheets on a quartz substrate is shown in Figure S8. After reduction of the TA-Fe/GO sheets, the absorption peaks around 300 and 550 nm derived from TA absorption and the charge transfer band between TA and Fe could still be observed, indicating the preservation of the TA-Fe films on rGO sheets.

The Raman spectra of the TA-Fe/rGO sheets in Figure 4b showed two characteristic D and G bands at 1352 and 1589 $cm^{-1}$, respectively. Before and after reduction of TA-Fe/Go sheets, the G band peak shifted from 1597 $cm^{-1}$ to 1589 $cm^{-1}$, indicating the reduction of GO according to previous reports.[24, 32] The D/G ratio is commonly increased after reduction of GO.[24, 33] The D/G ratio was increased from 1.03 for TA-Fe/GO to 1.09 for TA-Fe/rGO. It might be related to large quantities of structural defect by creation of small $sp^2$-carbon domains upon reduction of the GO[34] and the presence of TA-Fe films on graphene (Figure S9).

Furthermore, the reduction of GO-coated TA-Fe films was verified by XPS (Figures 4c and S10). The degree of reduction was evaluated by checking the C1s signals and their energy shift under the different conditions. The reduction of GO is known to lead to the removal of epoxy and hydroxyl groups on the GO surface. From the peak deconvolution results, the intensity ratios of O-C=O and C=C peaks decreased significantly compared to those of the TA-Fe/GO sheets. Therefore, The TA-Fe sheets embedded with GO sheets was reduced by hydrazine hydrate. For Fe atoms, Fe $2p_{1/2}$ and Fe $2p_{3/2}$ peaks were observed (Figure 4d), and the ratios of both intensities between $I$(Fe $2p_{3/2}$) and $I$(C1s) of TA-Fe/GO before and after reduction were kept constant (about 1:12), indicating the presence of TA-Fe films on the rGO sheets (Figure S11). From elemental analysis results, the C, H, and N percentage ratios of TA-Fe/rGO were 44.14, 2.15 and 6.39% and the remaining ratio was 47.32%, which contained the elements O and Fe. After chemical reduction, the C percentage ratio was increased from 40.31 to 44.14% because of the loss of oxygen-containing functional groups such as COOH and OH, indicating the reduction of GO sheets. The N elements

corresponded to residual hydrazine and reacted GO with hydrazine. From the XPS measurement, the existence of N elements was also confirmed (Figure S10).

Thermogravimetric (TG) curves from the GO, TA-Fe/GO, and TA-Fe/rGO sheets are shown in Figure S12. Graphene oxide is not stable, and the mass loss of below 200°C was due to the loss of adsorbed water- and oxygen-containing functional groups such as COOH and OH.[29] The mass loss of the TA-Fe/GO sheets below 200°C was also attributed to the removal of oxygen-containing functional groups. In contrast, the TA-Fe/rGO sheets showed no significant mass loss below 200°C, indicating the successful removal of oxygen-containing groups and absorbing water during chemical reduction. It is known that the main mass loss of TA is due to the decomposition of TA in the range from 200-300°C.[35] The TG curves of both TA-Fe/GO and TA-rFe/GO sheets were almost the same above 200°C, indicating the formation of the same materials after the removal of functional groups and absorbing water. These results present evidence for the successful reduction of GO-covered TA films.

To further clarify the reduction of GO sheets, the electrical conductivities of the TA-Fe/rGO sheets were measured and compared with those before reduction; i.e., TA-Fe/GO sheets. The resistance of the composite TA-Fe/rGO sheets was revealed in the range of several kilo to mega Ω by using a circuit tester. Figure 4e shows photographs of TA-Fe/rGO on a Au electrode. The *I-V* curve of this device was measured (Figure 4f). The linear *I-V* curve strongly indicated that the reduction of GO led to conductive rGO. On the other hand, for the TA-Fe/GO sheets, it was difficult to measure the conductivity of the TA-Fe/GO sheets due to high resistance in the device setup for this study. These results suggested that the TA-Fe network wrapped GO sheets were reduced, resulting in the formation of more conductive TA-Fe/rGO sheets.

The wrapping of the TA-Fe films has advantage for the modification of surface properties of rGO. To clarity the effect of TA-Fe films, we measured the contact angle of drop-cast films of TA-Fe/GO sheets before and after the reduction. The contact angles of TA-Fe/GO before and after reduction were 17.6° and 21.3°, respectively, resulting in a preservation of hydrophilic surface. On the other hand, the contact angles of GO before and after reduction were 36.3° and 71.2°, respectively, resulting in a change from hydrophilic to hydrophobic surface. These results indicated that the TA-Fe films can keep the hydrophilic property during the reaction on the wrapped GO.

The TA-Fe/GO sheets in this study is easy to handle and the dried film prepared from the spin-coating of TA-Fe/GO suspension and reduction is conductive, which can be used for electrode modification and device fabrication.

## Conclusions

We discussed the preparation of soft-wrapped GO sheets covered with $Fe^{III}$-polyphenol network film via the coordination of TA to $Fe^{III}$ ions. The wrapped sheet structures were examined using AFM, SEM, and TEM to form a uniform nanometer-sized wrapped film on the GO surface. X-ray photoelectron spectroscopy analysis showed that the Fe atoms were incorporated in the films on the GO surface. The TA-Fe/GO sheets were converted to TA-Fe/rGO sheets by chemical reduction. We believe TA-Fe/GO or TA-Fe/rGO sheets may be useful for applications in supercapacitor and electronics devices.

## Acknowledgments

This work was supported by the Ministry of Education, Culture, Sports, Science and Technology for a Grant-in-Aid for Young Scientists (B) (no. 50464152). MH acknowledges financial support from the Institute of Science and Engineering at Chuo University. We acknowledge Prof. Hideki Tanaka of Chuo University and Otsuka electronics Co., Ltd. for their support regarding the SEM observation and zeta potential measurement.

## Notes and references

Department of Applied Chemistry, Faculty of Science and Engineering, Chuo University, 1-13-27 Kasuga, Bunkyo-ku, Tokyo, Japan.
E-mail: mhaga@kc.chuo-u.ac.jp

Electronic Supplementary Information (ESI) available: Experimental details, additional Raman spectra, AFM, SEM, and XPS data. See DOI: 10.1039/c000000x/

1. Y. Zhu, S. Murali, W. Cai, X. Li, J. W. Suk, J. R. Potts and R. S. Ruoff, *Adv. Mater.*, 2010, **22**, 3906-3924.
2. D. R. Dreyer, S. Park, C. W. Bielawski and R. S. Ruoff, *Chem. Soc. Rev.*, 2010, **39**, 228-240.
3. D. R. Dreyer, A. D. Todd and C. W. Bielawski, *Chem. Soc. Rev.*, 2014,**43**, 5288-5301.
4. V. Georgakilas, M. Otyepka, A. B. Bourlinos, V. Chandra, N. Kim, K. C. Kemp, P. Hobza, R. Zboril and K. S. Kim, *Chem. Rev.*, 2012, **112**, 6156-6214.
5. K. Ariga, Y. Yamauchi, G. Rydzek, Q. Ji, Y. Yonamine, K. C. W. Wu and J. P. Hill, *Chem. Lett.*, 2014, **43**, 36-68.
6. X. Huang, X. Qi, F. Boey and H. Zhang, *Chem. Soc. Rev.*, 2012, **41**, 666-686.
7. Q. Ji, I. Honma, S.-M. Paek, M. Akada, J. P. Hill, A. Vinu and K. Ariga, *Angew. Chem. Int. Ed.*, 2010, **49**, 9737-9739.
8. K. Hu, M. K. Gupta, D. D. Kulkarni and V. V. Tsukruk, *Adv. Mater.*, 2013, **25**, 2301-2307.
9. Y. Wang, S. W. Tong, X. F. Xu, B. Özyilmaz and K. P. Loh, *Adv. Mater.*, 2011, **23**, 1514-1518.
10. Z. Li, J. Wang, X. Liu, S. Liu, J. Ou and S. Yang, *J. Mater. Chem.*, 2011, **21**, 3397-3403.
11. W. W. Liu, X. B. Yan and Q. J. Xue, *J. Mater. Chem. C*, 2013, **1**, 1413-1422.
12. X. Ou, L. Jiang, P. Chen, M. Zhu, W. Hu, M. Liu, J. Zhu and H. Ju, *Adv. Funct. Mater.*, 2013, **23**, 2422-2435.
13. R. R. Salunkhe, Y. Kamachi, N. L. Torad, S. M. Hwang, Z. Sun, S. X. Dou, J. H. Kim and Y. Yamauchi, *J. Mater. Chem. A*, 2014, **2**, 19848-19854.
14. J. Tang, R. R. Salunkhe, J. Liu, N. L. Torad, M. Imura, S. Furukawa and Y. Yamauchi, *J. Am. Chem. Soc.*, 2015, **137**, 1572-1580.
15. S. H. Hsu, C. T. Li, H. T. Chien, R. R. Salunkhe, N. Suzuki, Y. Yamauchi, K.-C. Ho and K. C. W. Wu, *Sci. Rep.*, 2014, **4**, 6983.
16. L. Q. Xu, W. J. Yang, K.-G. Neoh, E.-T. Kang and G. D. Fu, *Macromolecules*, 2010, **43**, 8336-8339.
17. Y. Wang, Z. Shi and J. Yin, *ACS Appl. Mater. Interfaces*, 2011, **3**, 1127-1133.
18. V. Kozlovskaya, S. Harbaugh, I. Drachuk, O. Shchepelina, N. Kelley-Loughnane, M. Stone and V. V. Tsukruk, *Soft Matter*, 2011, **7**, 2364-2372.



 

19. T. G. Shutava, S. S. Balkundi, P. Vangala, J. J. Steffan, R. L. Bigelow, J. A. Cardelli, D. P. O'Neal and Y. M. Lvov, *ACS Nano*, 2009, **3**, 1877-1885.
20. V. Kozlovskaya, E. Kharlampieva, I. Drachuk, D. Cheng and V. V. Tsukruk, *Soft Matter*, 2010, **6**, 3596-3608.
21. H. Ejima, J. J. Richardson, K. Liang, J. P. Best, M. P. van Koeverden, G. K. Such, J. Cui and F. Caruso, *Science*, 2013, **341**, 154-157.
22. J. Guo, Y. Ping, H. Ejima, K. Alt, M. Meissner, J. J. Richardson, Y. Yan, K. Peter, D. v. Elverfeldt, C. E. Hagemeyer and F. Caruso, *Angew. Chemie Int. Ed.*, 2014, **53**, 5546–5551.
23. M. A. Rahim, H. Ejima, K. L. Cho, K. Kempe, M. Müllner, J. P. Best and F. Caruso, *Chem. Mater.*, 2014, **26**, 1645-1653.
24. Y. Lei, Z. Tang, R. Liao and B. Guo, *Green Chem.*, 2011, **13**, 1655-1658.
25. X. Huang, J. Chen, H. Yu, R. Cai, S. Peng, Q. Yan and H. H. Hng, *J. Mater. Chem. A*, 2013, **1**, 6901-6907.
26. Y. Zhang, G. Chang, S. Liu, J. Tian, L. Wang, W. Lu, X. Qin and X. Sun, *Cat. Sci. Technol.*, 2011, **1**, 1636-1640.
27. Y. Zhang, S. Liu, W. Lu, L. Wang, J. Tian and X. Sun, *Cat. Sci. Technol.*, 2011, **1**, 1142-1144.
28. H. Zhao, J. Yang, L. Wang, C. Tian, B. Jiang and H. Fu, *Chem. Commun.*, 2011, **47**, 2014-2016.
29. D. C. Marcano, D. V. Kosynkin, J. M. Berlin, A. Sinitskii, Z. Sun, A. Slesarev, L. B. Alemany, W. Lu and J. M. Tour, *ACS Nano*, 2010, **4**, 4806-4814.
30. R.-Y. Liu and A.-W. Xu, *RSC Advances*, 2014, **4**, 40390-40395.
31. H. A. Becerril, J. Mao, Z. Liu, R. M. Stoltenberg, Z. Bao and Y. Chen, *ACS Nano*, 2008, **2**, 463-470.
32. S. Stankovich, D. A. Dikin, R. D. Piner, K. A. Kohlhaas, A. Kleinhammes, Y. Jia, Y. Wu, S. T. Nguyen and R. S. Ruoff, *Carbon*, 2007, **45**, 1558-1565.
33. D. Yang, A. Velamakanni, G. Bozoklu, S. Park, M. Stoller, R. D. Piner, S. Stankovich, I. Jung, D. A. Field, C. A. Ventrice Jr and R. S. Ruoff, *Carbon*, 2009, **47**, 145-152.
34. Z. Bo, X. Shuai, S. Mao, H. Yang, J. Qian, J. Chen, J. Yan and K. Cen, *Sci. Rep.*, 2014, **4**, 4684.
35. M. I. Popa, G. Lisa and N. Aelenei, *Polymer Bulletin*, 2008, **61**, 481-490.